Chalcogenide Letters Vol. 19, No. 7, July 2022, p. 493 - 501

Optimization of photonic crystal structure by FDTD method to improve the light extraction efficiency in silicon

N. B. Khairulazdan, P. S. Menon, A. R. Md. Zain, D. D. Berhanuddin*
National University of Malaysia (UKM), Institute of Microengineering and Nanoelectronics (IMEN), 43600 UKM Bangi, Selangor, Malaysia

Silicon photonics technology is on its last hurdle to complete the system with active research on enhancing the light extraction efficiency of silicon. Silicon has a very poor radiative emission efficiency due to its indirect bandgap, thus making the probability of radiative recombination to be very low. The periodic quantum confinement structures such as photonic crystals (PhCs) can be tailored to increase the radiative recombination probability at the desired wavelengths. In this paper, we have optimized the silicon photonic crystal (Si PhCs) parameters to obtain luminescence at silicon bandgap and telecommunication wavelength using FDTD method. The extraction of photons is mostly conquered in the silicon structure that has lattice constant, *a*: 480 nm with radius, *r*: 140 nm and *a*: 500 nm with *r*: 160 nm. We have also observed the emissive photon luminescence that emerges in the most stable state of optical communication wavelength at 1310 nm.

(Received March 13, 2022; Accepted July 26, 2022)

Keywords: Silicon photonics, Photonic crystals, FDTD, Photoluminescence, Light-emitting devices

1. Introduction

Traditionally, the idea of extracting and emitting light from the single crystal silicon structure has been considered impossible because of its indirect bandgap at 1.12eV which is equivalent to ~1100 nm wavelength.[1] Apart from the indirect bandgap issue, silicon is a promising material to build a variety of photonic devices. Compared to germanium (Ge), silicon has a larger bandgap which allows higher operating temperature.[2] It also has high thermal conductivity and optical damage threshold (~10x higher than GaAs). Besides, silicon has high third-order optical nonlinearities, a larger Kerr effect and the Raman effect is 1000 times stronger than those in silica fibre.[3] Various approaches have been attempted to try circumventing the bandgap limitation and transforming silicon as an optically active material. Among the successful and promising methods of emitting light from silicon are point defect centres,[4],[5] incorporation of quantum confined structures[6],[7] and introduction of rare earth element such as Erbium. Although impressive, these approaches have some shortcomings that hinder their use in telecommunications. The previous methods are either work only at low temperature in broad area devices, cannot be pumped electrically or emit at bandgap or shorter wavelengths. Commonly, there is three main wavelengths used for optical communication system are 850 nm, 1300 nm and 1550 nm.[8],[9],[10] Divers study have stated that the wavelength having the lowest attenuation and reduce the loss of signal strength during transmission of the light.[9]

Quantum confinement structures give rise to discrete energy levels that can help overcome the bandgap issue of silicon. Periodic structures such as photonic crystals (PhCs) can control the optical modes by evaluating the geometrical aspect such as the lattice constant and radius of each hole.[11] These PhCs properties have been studied to improve optoelectronic device performance such as optical biosensors, solar cells, and light-emitting devices.[12],[13],[14] The utilization of PhCs structure on silicon-on-insulator (SOI) has been a particular subject of interest in the field of silicon photonics to improve the emission. The introduction of photonic crystal (PhCs) in silicon

* Corresponding author: dduryha@ukm.edu.my
https://doi.org/10.15251/CL.2022.197.493

or SOI substrate increases the light extraction efficiency from thin light-emitting layers via light-matter interaction. If the light emission spectrally overlaps the leaky modes or guided resonance of PhCs, the light can cause these modes to be diffracted out of structure at a defined angle. The structure must be carefully designed, while considering all its physical properties including the spatial distribution of refractive index (RI). The photonic bandgap depends on the optical material properties which disallowed particular wavelength in periodic PhCs. The photonic bandgap depends upon crystal parameter such as lattice structure (hexagonal, square lattice, etc.), lattice constant *a*, radius of hole area *r*, filing ratio *f*, dielectric constant contrast, the polarization of wave and the direction of propagation.[15]

In this paper, the optimized structure to maximize the light extraction in silicon-based 2D PhCs at particular infrared and telecommunication wavelengths are presented using the finite-difference time-domain (FDTD) method. The various structure is analysed to improve and enhance the performance of silicon surface to extract the light as a device. The properties of PhC structure are numerically investigated by using the 3 Dimension (3D) Finite-difference time-domain (FDTD) method. The 2D PhCs are preferred especially in telecommunication technology compared to 3D PhCs due to less complex fabrication for future mass production while supporting the near-infrared and visible spectrum applications.[16] The geometrical parameters were varied to investigate its effect on luminescence intensity at a specific wavelength. The result of this study will assist in the future fabrication of silicon light-emitting devices with emission at room temperature, with wavelength compatible for telecommunication applications. As we introduce the PhCs in the Si substrate, the photonic bandgap of the Si will be altered depending on the parameters such as the lattice constants, type of the symmetry structure, filling factor along the plane wave and dielectric constant contrast.[17] The final condition of the band structure will determine which light can exhibit a certain frequency or wavelength in any direction within the material.

2. Methodology

The schematic of Si PhC is shown in Fig. 1. A hexagonal lattice array configuration on silicon on insulator (SOI) wafer was used throughout the study. The geometrical parameters were varied by considering two different lattice constant, *a*; 480 and 500 nm with different radius, *r* ranging between 100 to 200 nm. The SOI layer consists of Si with 220 nm thickness on a 3μm buffer oxide layer (SiO_2). These dielectric layers provide the best confinement for optical propagation through guiding layers, while providing isolation to the silicon layer. The lattice constant gap between two holes can induce a substantial local optical near field condition that interacts with incident light source to provide luminescence in SOI wafer. The parameters were chosen based on the previous study by A.Mahdavi *et al.*, they optimized the PhC structure with lattice constant, a = 480 nm with radius, r = 139 nm.[1] In this paper, the new finding is to compare with different a = 500 nm of the same radius range with selected paper. To select the best PhC structure, we use the referred value from A.Mahdavi's paper and add about ± 20 nm increment to prove the effectiveness of the structure according to a different radius of the PhC holes. The a = 500 nm probably going to have a different optimum radius, thus the varied range should be considered to be analysed.

In photonic crystals, the famous Maxwell's equations are used to study light propagation in photonic crystal structure. The propagation of light in a medium is governed by the four well-known Maxwell's equations given by Eq. (1) below;

$\nabla.B = 0$	Where each Si units defines as;
$\nabla.D = \rho$	B - Magnetic flux density in Tesla, T
$\nabla \times E + (\frac{\partial B}{\partial t}) = 0$	D - Electric flux density in Coulombs per square m, C/m^2
$\nabla \times H - (\frac{\partial B}{\partial t}) = J$ (1)	E - Electric field strength in Volt per meter, V/m
	H - Magnetic field strength in Ampere per meter, A/m
	P - Electric charge density in Coulombs per cubic meter, C/m^3
	J - Electric current density in Ampere per square meter, A/m^2

For most dielectric material, the magnetic permeability, μ_r is equal to 1, and the B = H thus gives the flux density, D = ε.E (where E is real (r)). The re-written Maxwell's Equations are express in Eq. (2);

$$\nabla.H = 0$$
$$\nabla.\varepsilon(r)E(r,t) = 0$$
$$\nabla \times E(r,t) + \frac{1}{c}\left(\frac{\partial H(r,t)}{\partial t}\right) = 0$$
$$\nabla \times H(r,t) - \frac{\varepsilon(r)}{c}\left(\frac{\partial E(r,t)}{\partial t}\right) = 0 \quad (2)$$

In addition, the harmonic mode of the E and H propagating in the dielectric medium are considered as zero, and later the H(r) and E(r) field components at t=0, the Maxwell's equation will become;

$$\nabla \times \left(\frac{1}{\varepsilon(r)} \nabla \times H(r)\right) = \left(\frac{\omega}{c}\right) H(r) \quad (3)$$

$$E(r) = \left[\frac{-ic}{\omega\varepsilon(r)}\right] \nabla \times H(r) \quad (4)$$

The Eq. (3) only have H(r) components which used for dielectic medium that consider the magnetic field of PhC and Eq. (4) also used to recover an electric field component, E(r) of Maxwell's equation. Both equation above are used to understand the basic concepts of photonic crystal structures.

The 3D Finite Difference Time Domain (FDTD) method is interesting technique because it provides both the spatial and temporal properties of the structure with a single calculation thus making it suitable for the analysis of many structures. The FDTD method from Lumerical software was used to analyse the luminescence enhancement obtain in Si PhCs. The FDTD method is the process of translating Maxwell's Equation into a form of approximation electromagnetic fields of any complex geometric structures and devices.[18] A method is a powerful tool for modelling nanoscale optical devices. It solves Maxwell's Equation directly without any physical approximation. Other than that, the method has also been able to estimate the exact numerical value in a complex geometric structure by confining the source in one small area of the surface.[19] This type of computational technique is very suitable for our proposed structure with a various range of parameters.

In the simulation setup, a one-cell area of the hexagonal lattice was set as a domain and perfectly matched layers (PML) are imposed in x and y axes to maximize the light source confinement in the FDTD area. The plane-wave light source in the x-axis was analyzed with broadband ranging between 900 to 1600 nm. The chosen range is in between near-infrared wavelength of light absorption and emission can occur in silicon surface. This broad wavelength is applied to monitor how many response peaks in one waveband at one time. The extraction of light through electric field intensity that inhibits silicon bandgap wavelength of 1100 nm and optical communication wavelength in between 1260 nm and 1360 nm were also monitored. Based on a

past study, they focus on resonance light peak at 1280 nm which match the important optical communication wavelength at 1300 nm of the silicon-based light-emitting devices.[20] For band structure, the simulation was set up using the same Lumerical software by using the PhCs with high symmetry structure of hexagonal array in the first Brillouin Zone; k_x, k_y = 0. The reciprocal lattice of the PhCs structure resulting in the band diagram by marching around the perimeter of the irreducible Brillouin Zone. The k wavevector consists of the transverse electric (TE) and transverse magnetic (TM) mode for each optimum radius in both selected lattice constants. The diagram was generated by using 15 points sweep of each k-vector of the reciprocal lattice applied.

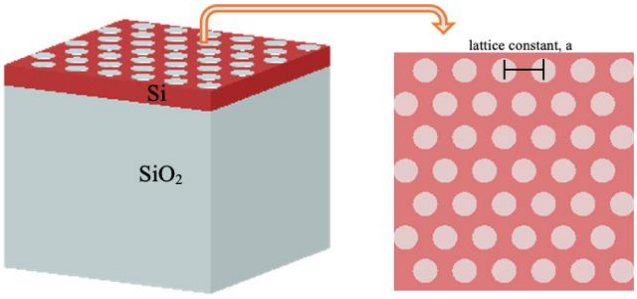

Fig. 1. Schematic diagram silicon photonic crystals using SOI wafer.

3. Results and Discussion

3.1. Optimizing radius in 480 nm & 500 nm lattice constant, a

As for optimizing the PhC structures, we varied the radius, r for each lattice constant, a 480 nm & 500 nm as shown in fig. 2 and Table 1. In fig. 2(a) we can see that the graph compared the luminescence intensity appear in unpatterned Si and for both *a* = 480 nm and *a* = 500 nm with the radius range of 100 to 200 nm. The *a* = 480nm and 500 nm that give the highest value of excitation peak appear at *r* = 140 nm with 0.8781×10^6 intensity peak and *r* = 160 nm with 0.8957×10^6 respectively. Next, the comparison of Si PhC with unpatterned Si have been calculated which give about 49.77% and 52.77% enhancement for *a* = 480 nm and 500 nm accordingly. The percentage value is calculated by finding different values between the highest intensity value for each lattice constant, a with unpatterned Si value then divided by the unpatterned value. Besides, the normalized intensity also was determined with the result value lies between 0 to 1, which the highest one will be value of 1 as shown in Fig. 2(b). The purposed of the normalized graph is to summarise the best structure of Si PhC with optimum radius of the highest normalized value. The equation for normalization is derived by initially deducting the min value from the variable to be normalized. The min value is deducted from the maximum value and the previous result is divided by the latter. Mathematically, the normalized equation is represented as (5);

$$x(normalized) = \frac{(x - x(min))}{(x(max) - x(min))} \tag{5}$$

As we introduced the Si PhC with *a* = 480 nm starting from *r* = 100 to 200 nm, the highest intensity peak with a value of 1 lies at *r* = 140 nm as denoted in Table 1. This condition gives the same result as reference paper that indicate a radius around *r* ~139 nm was having the best extraction of light.[1] In the case for *a* = 500 nm, the best radius, *r* with a value of 1 for the highest intensity peak happened at *r* = 160 nm also refer to Table 1. From my point of view, the situation occurs due to less total internal reflection on PhC surface for both lattice gaps and all in-plane modes are more easily diffracted to the surround of Si surface. As we increase the lattice constant, *a*, the higher the luminescence can occur with suitable radius, *r* of PhC hole.[1] However, the intensity will eventually drop when the radius is too big thus reducing the confinement capability of the structure.

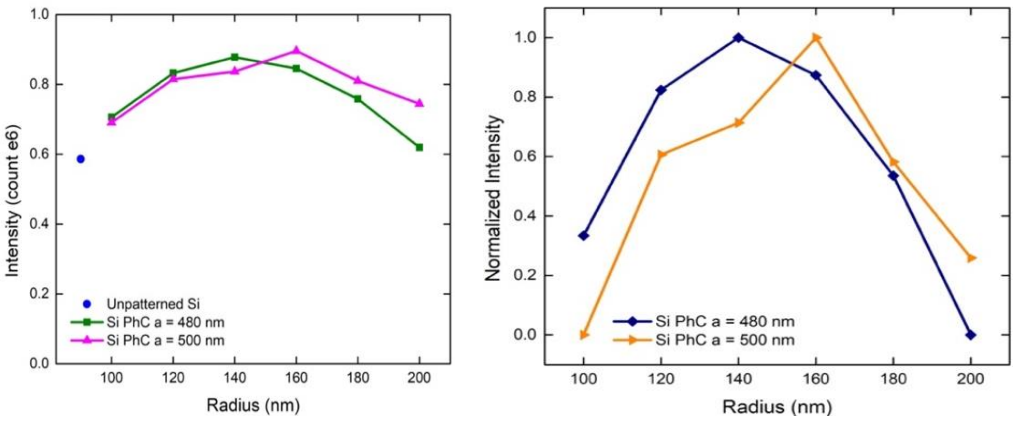

(a) *(b)*

Fig. 2. The graph comparison of (a) luminescence intensity peak (b) normalized luminescence intensity for Si PhCs having a a = 480 nm and 500 nm with r = 100 to 200 nm.

Table 1. The intensity value and normalized intensity for a; 480 nm and 500 nm with 100 < r < 200.

Radius, *r* (nm)	Intensity value (e6)		Normalized Intensity value	
	a = 480 nm	*a* = 500 nm	*a* = 480 nm	*a* = 500 nm
100	0.7059	0.6911	0.3338	0.0000
120	0.8326	0.8151	0.8240	0.6061
140	0.8781	0.8371	1.0000	0.7136
160	0.8454	0.8957	0.8735	1.0000
180	0.7581	0.8102	0.5358	0.5821
200	0.6196	0.7441	0.0000	0.2590

3.2. The resonance peaks at the desired wavelength

Fig. 3 shows the emission peaks emerging in between 900 to 1600 nm wavelength with a few resonance peaks gain in both *a* = 480 nm and 500 nm structures. These specific PhC structures were considered due to ability to extract the light in the telecommunication band as well as altering the photonic bandgap of Si PhCs. The PhC with *a* = 480 nm is observed to have peaks at 1017 nm, 1313 nm, 1478 nm and 1504 nm. The structure's peak at 1313 nm is within the telecommunication wavelength range but no light extraction peak observe at the Si bandgap wavelength of ~1100 nm. In the case of *a* = 500 nm, two distinguish peaks can be seen at 1097 nm and 1308 nm. This structure has light extracted within the Si Bandgap and at telecommunication band (~1300 nm). The peak at 1308 nm has the highest intensity compared to the other peaks in the spectrum. The resonance peaks in between the wavelength range for *a* = 500 nm with *r* = 160 nm has realtively higher values as compared to peaks for *a* = 480 nm with *r* = 140 nm. The resonance peak position and intensity are caused by the loss radiation of light in the PhCs structure in between the lattice array, fill factor and also dielectric of constant material. Therefore, by adjusting those parameters, the lights can be extracted in the selected wavelength. The PhCs structure of *a* = 500 nm with *r* = 160 nm has better potential to perform as a light-emitting device since it can extract light in both Si bandgap and telecommunication wavelengths.

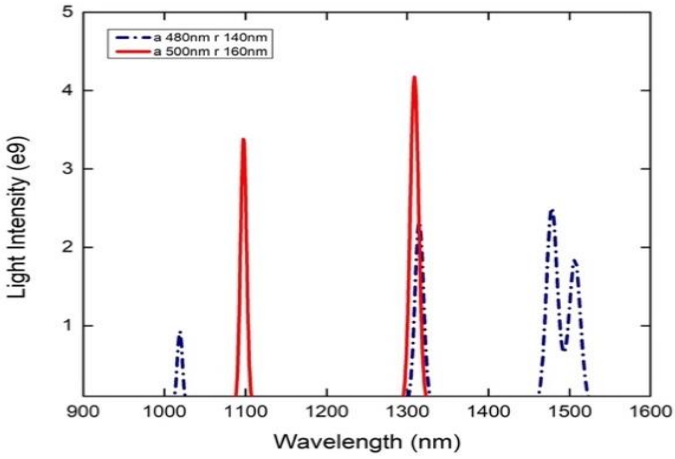

Fig. 3. The emission peak intensity as a function of wavelength for PhCs structures with lattice constant at a = 480 nm, r = 140 nm (dotted blue line) and a = 500 nm, r = 160 nm (red line).

Table 2. The resonance peak intensity value appear at wavelength range 900 nm to 1600 nm.

PhC structure	Wavelength (nm)	Resonance Peak Intensity (e9)
a = 480 nm, r = 140 nm	1017	0.8
	1313	2.3
	1478	2.5
	1504	1.7
a = 500 nm, r = 160 nm	1097	3.2
	1308	4.1

3.3. Band structure diagram corresponding to the symmetry hexagonal arrays of PhCs

The band energy diagrams for both optimized structures of *a* = 480 nm, *r* = 140 nm and *a* = 500 nm, *r* = 160 nm are shown in the Fig. 4(a) and Fig. 4(b), respectively. The yellow line indicates the wavelength range of 1100 nm ± 50 nm (Si bandgap energy). In Fig. 4(a), the gap has no clear energy level especially within the classic silicon intrinsic bandgap, reflecting in the absence of silicon bandgap peak and lower peak intensities as compared to the other structure shown in previous figure. In contrast, Figure 4(b) has more energy or frequency levels available, thus giving higher probability of radiative recombination to exist in the indirect bandgap energy area and increase the light intensities of the resonance peaks. The energies that can generate inside the lattice arrays are demonstrated in the band diagram from k (Gamma-M-K-Gamma) vectors.

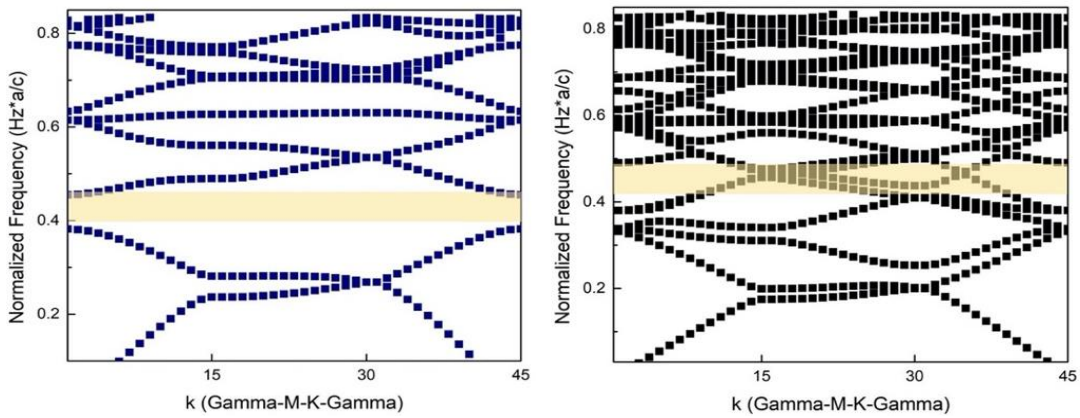

Fig. 4. Band structure of lattice constant (a) a = 480 nm, r = 140 nm and (b) a = 500 nm, r = 160 nm.

3.4. Electric field enhancement at 1100 nm and 1310 nm

Further observation was carried out by examining the electric field enhancement and light confinement at silicon bandgap emission, 1100 nm and telecommunication wavelength, 1310 nm. The surface area of light extraction was increase to allow more electrons to excite at a higher wavelength up to the optical communication band. In this section, Si PhCs at a = 480 nm and 500 nm were compared separately for the wavelength of 1100 nm and 1310 nm. From the previous results, we investigated the electric field profile for a selected structure which are a = 480 nm; r =140 nm and a =500 nm, r =160 nm as shown in Fig. 5 and Fig. 6, respectively in xz (a,c) and xy (b,d) plane. Most of the light gets confined at 1310 nm as shown in Fig. 5(c,d) while Fig. 5(a,b) show weak light confinement at 1100 nm. Further improvement can be seen for a = 500 nm and r = 160 nm, where the intensity of light is higher even in the structure with emission at 1100 nm as shown in Fig. 6(a,b) and light most likely to confine at 1310 nm in Fig. 6(c,d). The incident light that strikes the surface is mostly concentrated at the PhCs area where the structure will help to amplify the incoming EM excitation field in between them.[21] By having PhCs as the light extraction medium, less total internal reflection occurs and it can be easily diffracted to the surrounding medium.[22],[23]

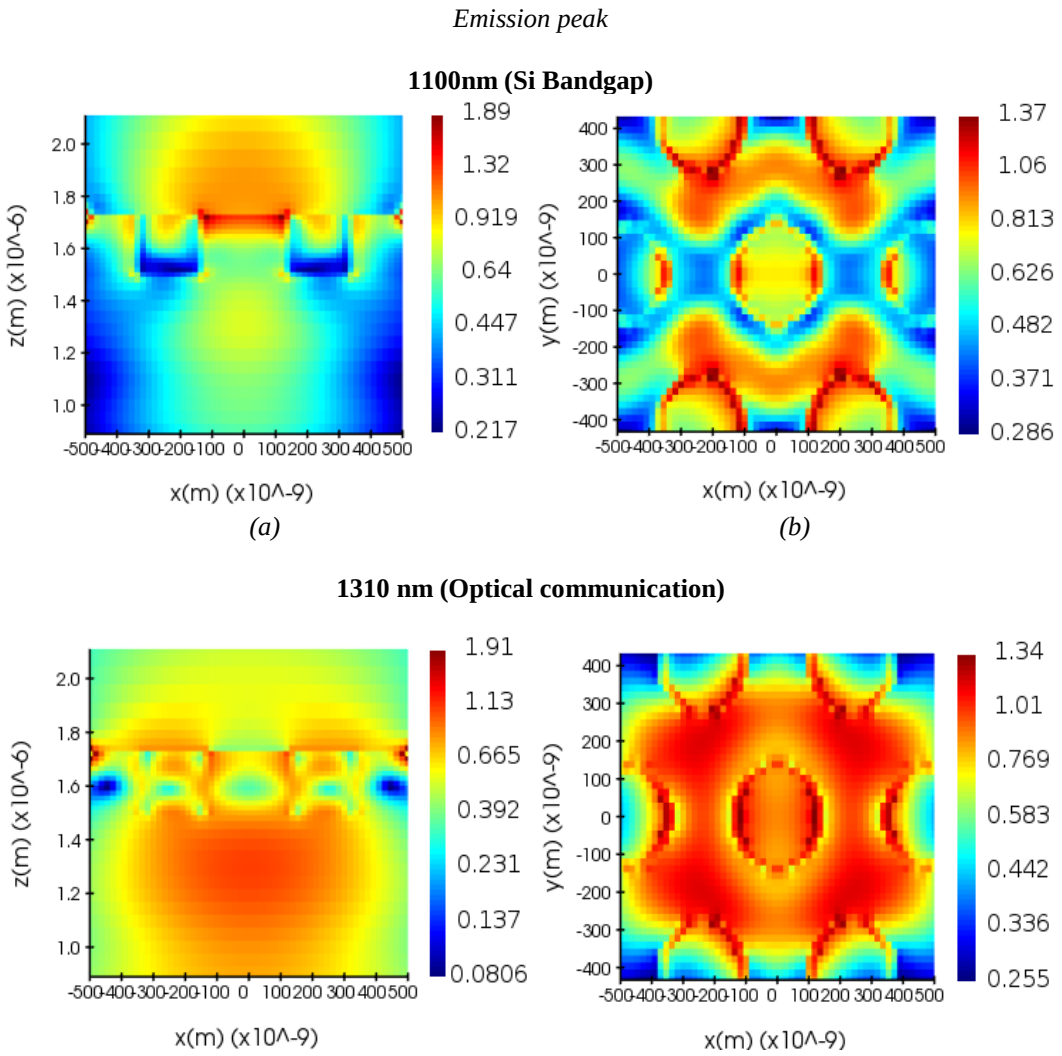

Fig. 5. The electric field intensity (a)(b) in xz planes, (c)(d) in xy planes of Si PhCs configuration at 1100 nm and 1310 nm wavelength for a = 480 nm, r = 140 nm.

Emission peak

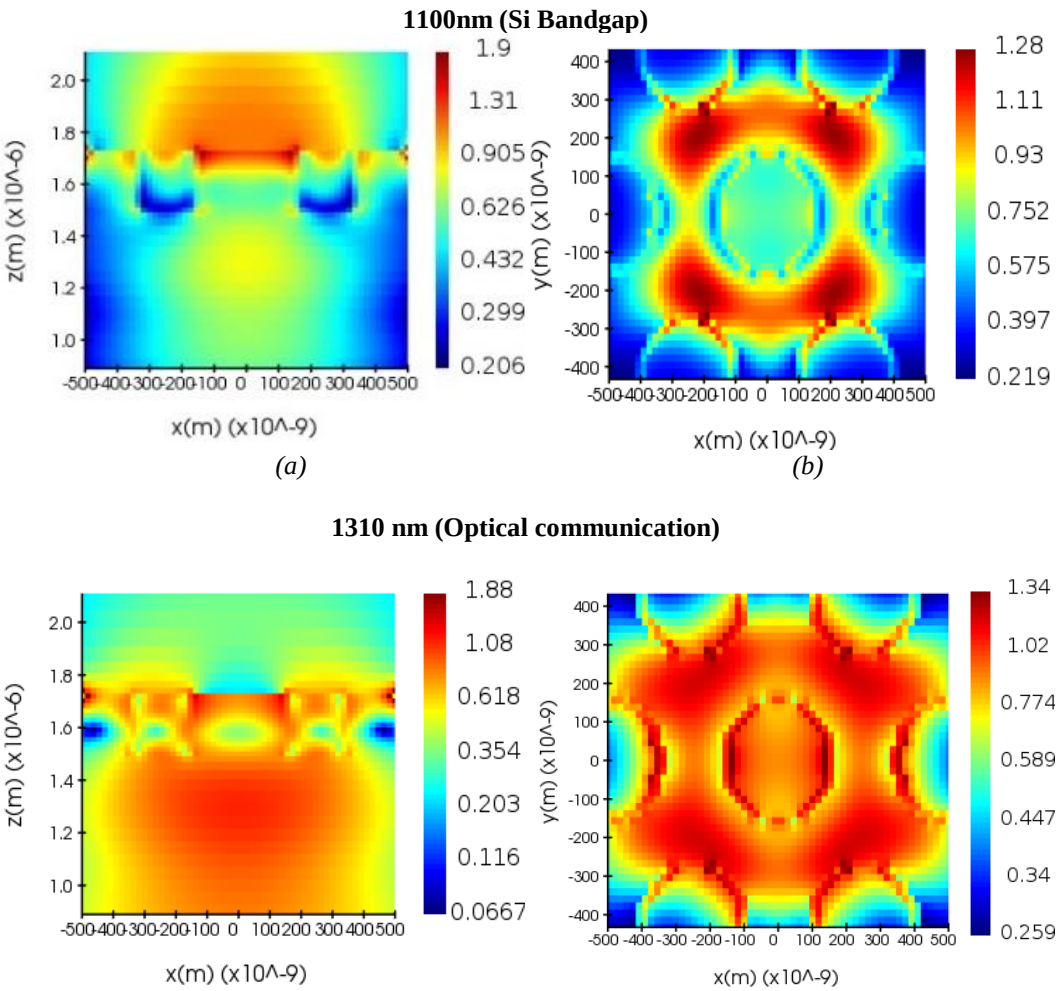

Fig. 6. The electric field intensity (a)(b) in xz planes, (c)(d) in xy planes of Si PhCs configuration at 1100 nm and 1310 nm wavelength for a = 500 nm, r = 160 nm.

4. Conclusions

We have demonstrated Si PhCs structures with tailored peak excitation for lattice constant *a*, at 480 nm and 500 nm. The optimized radius *r*, for *a* at 480 and 500 nm to obtain the highest light extraction are 140 nm and 160 nm, respectively. The band structure and the light intensity peak indicate that *a* = 500 nm with *r* = 160 nm is a better parameter as compared to structure with *a* =480 nm, *r* =140 nm as it can extract light in both Si band gap and telecommunication wavelength with greater intensity of light. The electric field shows very stable light confinement in optical communication wavelength at 1310 nm. The spectrum can be modulated in the desired band by varying the geomatic design parameter such as the thickness, lattice constant *a*, and radius, *r* of the holes. These results are important for further Si PhCs device fabrication as one of the elements in light-emitting devices to complete the all Si-based photonic integrated system.

Acknowledgements

The authors acknowledge the Ministry of Education for financial support under the Fundamental Research Grant Scheme FRGS/1/2018/STG07/UKM/02/15 and Universiti Kebangsaan Malaysia under Grant GUP-2019-072.

References

[1] A. Mahdavi, G. Sarau, J. Xavier, T. K. Paraïso, S. Christiansen, F. Vollmer, Sci. Rep., vol. 6, pp. 1-6, 2016; https://doi.org/10.1038/srep25135

[2] A. Irrera et al., Phys. E Low-Dimensional Syst. Nanostructures, vol. 38, no. 1-2, pp. 181-187, 2007; https://doi.org/10.1016/j.physe.2006.12.019

[3] R. Soref, IEEE J. Sel. Top. Quantum Electron., vol. 12, no. 6, pp. 1678-1687, 2006; https://doi.org/10.1109/JSTQE.2006.883151

[4] C. Beaufils et al., Phys. Rev. B, vol. 97, no. 3, pp. 69-71, 2018; https://doi.org/10.1103/PhysRevB.97.035303

[5] D. D. Berhanuddin, N. E. A. Razak, M. A. Lourenço, B. Y. Majlis, K. P. Homewood, Sains Malaysiana, vol. 48, no. 6, pp. 1251-1257, 2019; https://doi.org/10.17576/jsm-2019-4806-12

[6] L. Ondič, M. Varga, I. Pelant, J. Valenta, A. Kromka, R. G. Elliman, Sci. Rep., vol. 7, no. 1, pp. 1-8, 2017; https://doi.org/10.1038/s41598-017-05973-y

[7] Z. Ni, S. Zhou, S. Zhao, W. Peng, D. Yang, X. Pi, Mater. Sci. Eng. R Reports, vol. 138, no. June, pp. 85-117, 2019; https://doi.org/10.1016/j.mser.2019.06.001

[8] A. M. Alatwi, A. N. Zaki Rashed, Indones. J. Electr. Eng. Comput. Sci., vol. 21, no. 1, pp. 278-286, 2021; https://doi.org/10.11591/ijeecs.v21.i1.pp278-286

[9] A. M. Alatwi, A. N. Z. Rashed, I. A. A. El-Aziz, Telkomnika (Telecommunication Comput. Electron. Control., vol. 19, no. 2, pp. 380-389, 2021; https://doi.org/10.12928/telkomnika.v19i2.16871

[10] F. Adel, I. Chaqmaqchee, S. Abdulsamad, A. Salh, M. Faeq, M. Sabri, Zanco J. Pure Appl. Sci., vol. 32, no. 2, 2020; https://doi.org/10.21271/zjpas.32.2.9

[11] J. D. Joannopoulos, P. R. Villeneuve, S. Fan, Nature, vol. 386, no. 6621. pp. 143-149, 1997; https://doi.org/10.1038/386143a0

[12] Z. Zhou, B. Yin, J. Michel, Light Sci. Appl., vol. 4, no. 11, pp. 1-13, 2015; https://doi.org/10.1038/lsa.2015.131

[13] X. Sheng, L. Z. Broderick, L. C. Kimerling, Opt. Commun., vol. 314, pp. 41-47, 2014; https://doi.org/10.1016/j.optcom.2013.07.085

[14] J. E. Baker, R. Sriram, B. L. Miller, Lab Chip, 2015; https://doi.org/10.1039/C4LC01208A

[15] L. N. Quan, J. Kang, C. Z. Ning, P. Yang, Chem. Rev., vol. 119, no. 15, pp. 9153-9169, 2019; https://doi.org/10.1021/acs.chemrev.9b00240

[16] D. G. Popescu P. Sterian, "FDTD analysis of photonic crystals with square and hexagonal symmetry," vol. 2, no. 2, pp. 1-5, 2011.

[17] C. P. Mavidis et al., Phys. Rev. B, vol. 101, no. 23, p. 235309, 2020; https://doi.org/10.1103/PhysRevB.101.235309

[18] B. Fomberg, "Some Numerical Techniques for Maxwell's Equations in Different Types of Geometries," vol. 9810751, pp. 265-299, 2003; https://doi.org/10.1007/978-3-642-55483-4_7

[19] J.-W. Kim et al., Opt. Express, vol. 22, no. 1, p. 498, 2014; https://doi.org/10.1364/OE.22.000498

[20] D. D. Berhanuddin, M. A. Lourenço, R. M. Gwilliam, K. P. Homewood, Adv. Funct. Mater., vol. 22, no. 13, pp. 2709-2712, 2012; https://doi.org/10.1002/adfm.201103034

[21] K. Jung, Bull. Korean Chem. Soc., vol. 41, no. 12, pp. 1128-1129, 2020; https://doi.org/10.1002/bkcs.12131

[22] A. S. M. Mohsin, M. Mobashera, A. Malik, M. Rubaiat, M. Islam, J. Opt., vol. 49, no. 4, pp. 523-532, 2020; https://doi.org/10.1007/s12596-020-00656-w

[23] K. Bergenek et al., Appl. Phys. Lett., vol. 93, no. 4, pp. 1-4, 2008; https://doi.org/10.1063/1.2963030